Uncovering Early Galaxy Evolution in the ALMA and JWST Era
Proceedings IAU Symposium No. 352, 2019
E. da Cunha, J. Hodge, J. Afonso, L. Pentericci & D. Sobral, eds.

doi:10.1017/S1743921319008895

More than star formation: High-*J* CO SLEDs of high-*z* galaxies

Chelsea E. Sharon[1], Reni Chng[1], Kebron K. Gurara[1], Axel Weiß[2], Jeremy Darling[3], Dominik Riechers[4] and Carl Ferkinhoff[5]

[1]Yale-NUS College, Singapore, 138527, Singapore
email: chelsea.sharon@yale-nus.edu.sg

[2]Max-Planck-Institut für Radioastronomie, Auf dem Hügel 69 D-53121 Bonn, Germany

[3]Center for Astrophysics and Space Astronomy, Department of Astrophysical and Planetary Sciences, University of Colorado, Boulder, CO 80309-0389, USA

[4]Department of Astronomy, Cornell University, Ithaca, NY 14853, USA

[5]Physics Department, Winona State University, Winona, MN 55987, USA

Abstract. Theoretical work suggests that AGNs play an important role in quenching star formation in massive galaxies. In addition to molecular outflows observed in the local universe, emission from very high-*J* CO rotational transitions have been a key piece of evidence for AGN directly affecting the molecular gas reservoirs that fuel star formation. However, very few observations exist of CO rotational lines past the peak of the CO spectral line energy distribution (SLED) for galaxies in the early universe. Here we present new ALMA observations of high-*J* CO rotational lines (from CO(5–4) to CO(16–15)) in six $z > 2$ IR-bright systems, including several sources not known to contain a strong AGN for comparison. We detect significant amounts of high-excitation CO emission that suggests the presence of energy sources beyond UV-heating.

Keywords. Galaxies: high-redshift, Galaxies: active, Galaxies: star formation, ISM: molecules

1. Background

Explaining the mismatch between the observed number of massive galaxies and the number predicted by ΛCDM cosmology has largely relied on feedback from active galactic nuclei (AGNs) to suppress star formation (for a review, see Fabian 2012). However, the exact AGN feedback mechanisms and whether they are sufficient to quench star formation are still debated. Modes of AGN feedback can largely be classified as either indirect, where the radio jet prevents accretion of new gas onto the galaxy (i.e. kinetic, jet, radio, or maintenance mode feedback; e.g., Kereš *et al.* 2005), or direct, where the AGN removes gas already present in the galaxy or otherwise prevents that gas from forming stars (i.e. radiative, wind, or quasar mode feedback; e.g., Silk & Rees 1998). While evidence for indirect AGN feedback exists in hot X-ray gas halos (e.g., Bîrzan *et al.* 2012), concerns about the duty cycles of AGNs' radio phase remain (e.g., Shabala *et al.* 2008). Indirect AGN feedback also does not suppress star formation in galaxies with existing large molecular gas reservoirs (e.g., submillimeter galaxies; SMGs; e.g., Casey *et al.* 2014). Studies of direct AGN feedback have largely focussed on the ubiquity of observed outflows (e.g., Veilleux *et al.* 2005), although it is challenging to distinguish between AGN-driven and starburst-driven winds (e.g., Diamond-Stanic *et al.* 2012; Gowardhan *et al.* 2018), and it is unclear what fraction of winds' mass eventually return to the galaxy. Molecular gas outflow rates have been recently confirmed to correlate with AGN luminosity at low redshift (Cicone *et al.* 2014), but similar observations are too observationally expensive

Table 1. Summary of observations & spectral line fits

Source	Class[a]	$z_{\rm fiducial}$	Spectral Line	$z_{\rm fit}$	FWHM (km s^{-1})	$S\Delta v^b$ Jy km s^{-1}
BR 1202–0725 North	SMG	4.695	CO(13–12)	4.6932 ± 0.0005	1314 ± 64	3.0 ± 0.3
			CO(14–13)	4.6931 ± 0.0008	1301 ± 98	1.9 ± 0.2
BR 1202–0725 South	AGN	4.695	CO(13–12)	4.6944 ± 0.0004	348 ± 47	0.61 ± 0.08
			CO(14–13)	4.6948 ± 0.0005	423 ± 70	0.54 ± 0.07
Cloverleaf	AGN+L	2.560	CO(11–10)	2.55785 ± 0.00005	412 ± 9	33 ± 3
SMM J04431+0210	SMG	2.510	CO(5–4)	2.5082 ± 0.0008	360 ± 160	0.83 ± 0.23
			CO(8–7)	2.5084 ± 0.0003	287 ± 59	0.82 ± 0.13
SMM J14011+0252	SMG	2.565	CO(11–10)	2.5651 ± 0.0002	136 ± 33	0.43 ± 0.08
MG 0751+2716	AGN+L	3.200	CO(10–9)	3.1992 ± 0.0005	670 ± 84	7.3 ± 0.9
			CO(11–10)	3.1996 ± 0.0003	560 ± 52	4.1 ± 0.5
PSS J2322+1944[c]	AGN+L	4.119	CO(15-14)	4.1206 ± 0.0003	225 ± 41	0.74 ± 0.11
			CO(16-15)	4.1199 ± 0.0001	227 ± 55	0.80 ± 0.13
			OH 1835 GHz		314 ± 15	2.6 ± 0.3
			OH 1838 GHz			2.9 ± 0.3

[a]Indicates whether the source contains an AGN or is a SMG. "L" denotes sources that are strongly lensed.
[b]Uncertainties include statistical and assumed 10% flux calibration uncertainties combined in quadrature.
[c]The CO(16–15) line and two OH lines were fit simultaneously. The line separations were held fixed while fitting a global redshift. The two CO lines were constrained to have the same FWHM.

near the peak epoch of cosmic star formation (e.g., Madau & Dickinson 2014) and black hole accretion (e.g., Delvecchio *et al.* 2014), where most AGN feedback might be expected. At high redshift, detections of molecular outflows are often detected in less commonly studied species (such as CH^+ or OH in absorption; e.g., Falgarone *et al.* 2017; Spilker *et al.* 2018) that are challenging to convert into mass outflow rates.

It may be possible that correlations between CO excitation and AGN strength will reveal direct modes of AGN feedback. IR-bright AGN are known to produce CO SLEDs that peak near $J_{\rm upper} \sim 7$ (e.g., Weiß *et al.* 2007), while starburst-dominated galaxies like SMGs have CO SLEDs that peak near $J_{\rm upper} \sim 5$ (e.g., Carilli & Walter 2013). While initial systematic differences in low-J CO line ratios between SMGs and AGN (e.g., Swinbank *et al.* 2010; Harris *et al.* 2010; Ivison *et al.* 2011; Danielson *et al.* 2011; Riechers *et al.* 2011; Thomson *et al.* 2012) were not statistically significant in larger samples (Sharon *et al.* 2016), a more quantitative classification of AGN strength based on mid-IR spectral features suggests systematically higher excitation CO line ratios across the entire SLED for AGN (albeit with limited statistical power; Kirkpatrick *et al.* 2019). Looking for evidence of AGN feedback via CO excitation not only probes the fraction of the molecular gas affected by the AGN, but can also constrain how the AGN interacts with the gas (for example, via X-ray or shock heating; e.g., van der Werf *et al.* 2010; Meijerink *et al.* 2013). Constraining X-ray and shock heating requires observing very high-J CO lines, and there are few published observations of $J_{\rm upper} > 8$ lines at high redshift (Weiß *et al.* 2007; Riechers *et al.* 2013; Gallerani *et al.* 2014; Tuan-Anh *et al.* 2017; Oteo *et al.* 2017; Yang *et al.* 2017; Cañameras *et al.* 2018; Stacey & McKean 2018).

2. Observations & Results

In order to explore the prevalence of AGN-affected molecular gas and look for evidence of AGN feedback, we observed several high-J CO lines in a sample of $z > 2$ galaxies. We selected high-z galaxies accessible from Atacama Large Millimeter/submillimeter Array (ALMA) that either (a) already have a $J_{upper} > 9$ detection indicating that there is a high-excitation component that needs to be characterized more accurately, or (b) have an existing CO SLED that includes both the CO(1–0) and CO(7–6) line to aid

https://doi.org/10.1017/S1743921319008895 Published online by Cambridge University Press

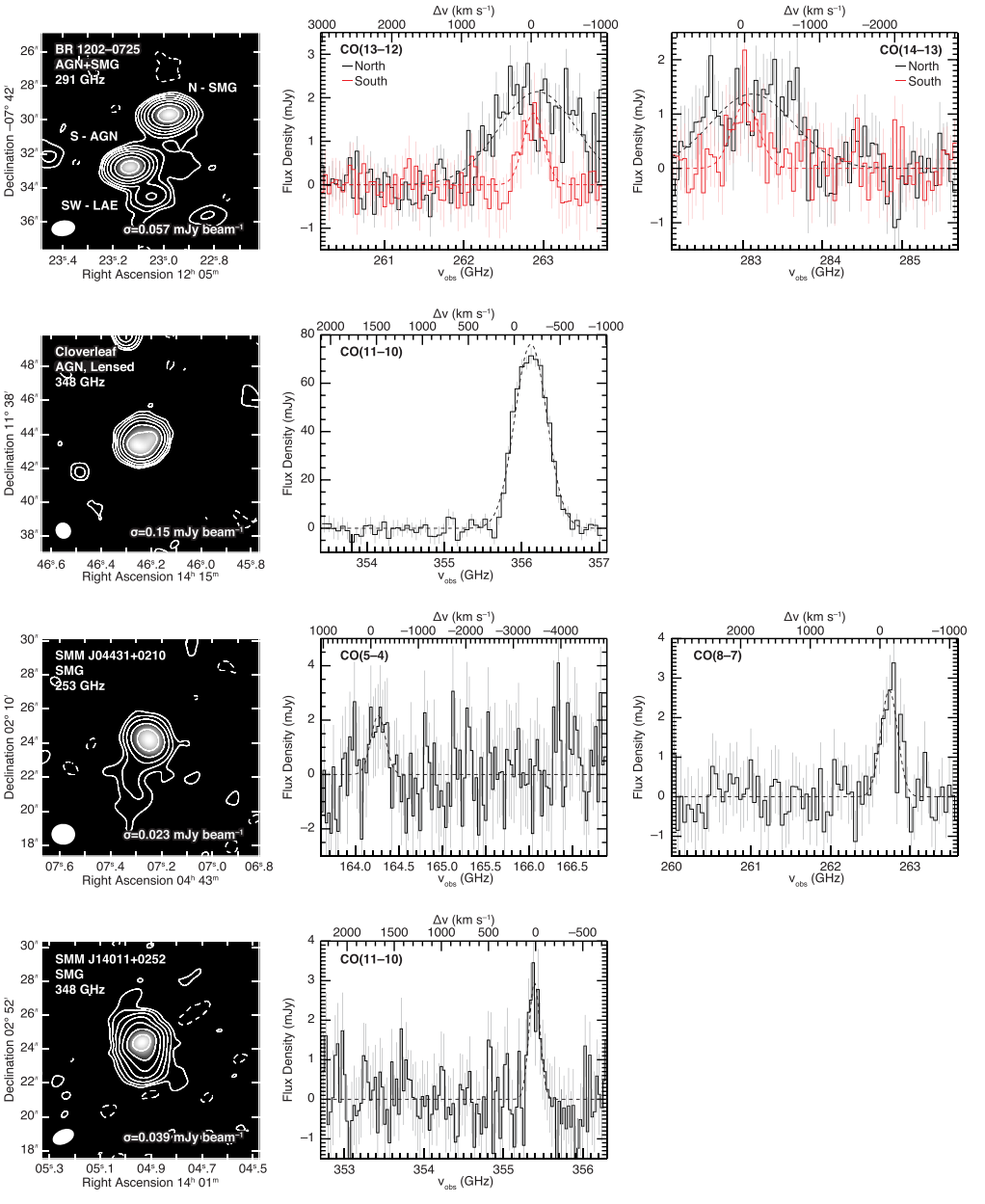

Figure 1. Continuum maps (left column) and continuum-subtracted spectra (middle and right columns) for our ALMA observations. We show the continuum maps from the higher frequency observations in cases where we observe multiple CO lines. Contours are powers of two times the map noise (i.e., $\pm 2\sigma$, $\pm 4\sigma$, $\pm 8\sigma$, etc.); negative values are dashed and the map noise is given in the lower right corner. The beam FWHM is shown in the lower left corner. For the spectra, the vertical bars show the $\pm 1\sigma$ statistical uncertainty in each channel. Dashed lines show the best-fit Gaussian line profile. The velocity axis is calculated relative to the fiducial redshift listed in Table 1. For BR 1202–0725, we show the spectra for the northern SMG in black and the southern AGN in red; since we do not detect significant line emission from the SW Lyman-α emitter we do not show its spectra. Note that SMM J14011+0252 is only weakly lensed.

https://doi.org/10.1017/S1743921319008895 Published online by Cambridge University Press

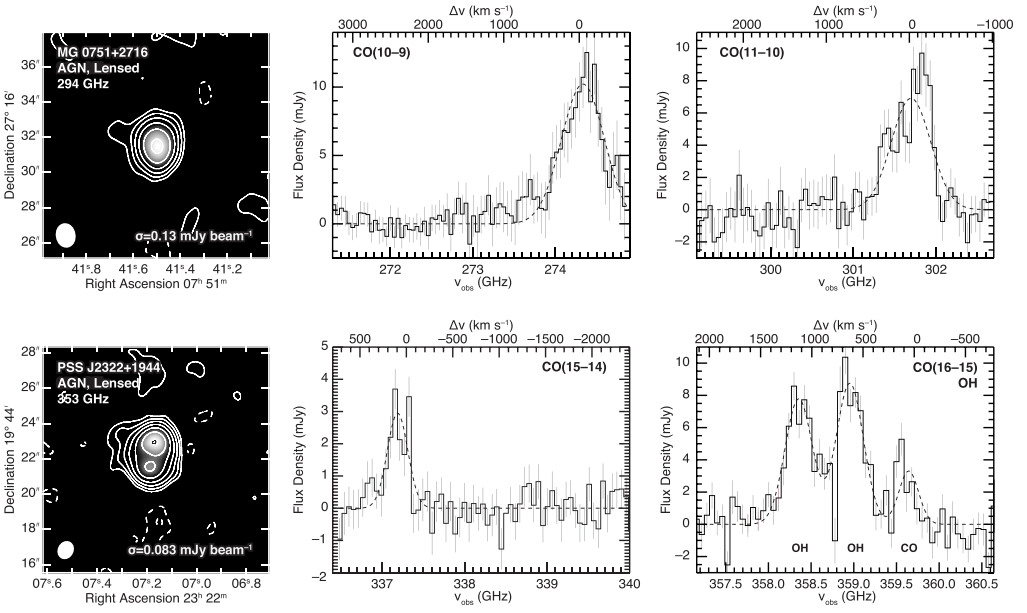

Figure 1. (Cont.)

estimates of the higher-J line strengths. We observed the next 1–2 higher-J CO lines during ALMA Cycle 5 (PID: 2017.1.00963.S). In addition to known high-z AGN, we also targeted several SMGs that are expected to be starburst-dominated in order to provide a baseline comparison sample for the effects of star formation alone on gas heating. For one target, we also observed a more moderate-excitation CO line in order to help fill in the SLED. For a complete list of targets and observed CO lines, see Table 1.

We show continuum maps and continuum-subtracted spectra in Figure 1. We detected all observed CO lines, although the detections of the CO(5–4) line for SMM J04431+0210 and the CO(16–15) line for PSS J2322+1944 are marginal ($\sim 5\sigma$ peak detections in the integrated line maps). In addition, for PSS J2322+1944, we detected the OH $^2\Pi_{1/2}$ $(3/2-1/2)$ doublet at 1835/1838 GHz. We also detected continuum from the Lyman-alpha emitter closely aligned with BR 1202–0725, but did not detect any significant CO emission.

3. Implications

While we have not yet compared the CO observations to radiative transfer models, the significant high-excitation CO emission in the AGN-dominated sources suggests there are additional heating mechanisms that must be considered (Fig. 2; however, one must be wary of differential lensing; e.g., Serjeant 2012). Many of these sources' SLEDs fall above the envelope for sources from the local *Herschel* Comprehensive (U)LIRG Emission Survey sample that *requires* an additional excitation mechanism, such as mechanical shocks and/or heating from X-rays or cosmic rays (Rosenberg *et al.* 2015). However, the differences in line ratios may be partially explained by the cosmic microwave background, particularly for the lower excitation SMGs and $z \sim 5$ sources (e.g., da Cunha *et al.* 2013). Only two sources (BR 1202–0725 North from this sample, and MG 0414 from Stacey & McKean 2018) show larger line FWHMs at higher-J (their lower-J CO FWHMs are ~ 300–$700\,\mathrm{km\,s^{-1}}$; Omont *et al.* 1996; Barvainis *et al.* 1998; Carilli *et al.* 2002; Salomé *et al.* 2012) suggesting they trace a dynamically distinct region.

https://doi.org/10.1017/S1743921319008895 Published online by Cambridge University Press

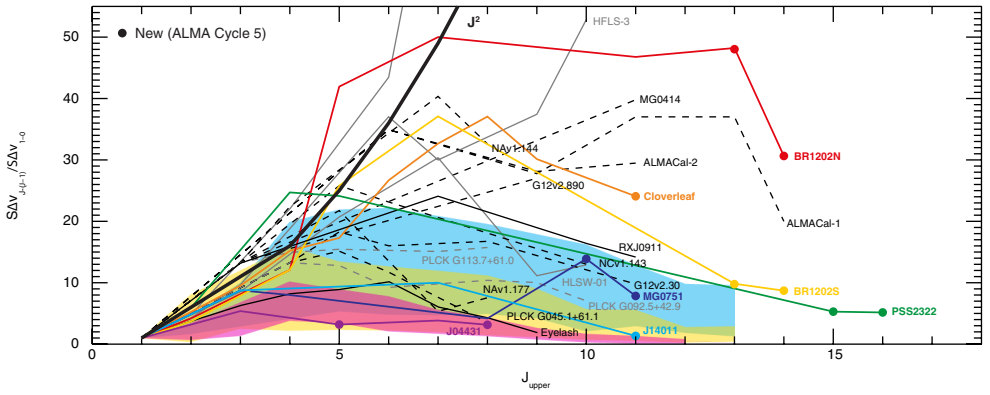

Figure 2. CO SLEDs for our sample (colored lines with symbols for new ALMA observations) normalized by the CO(1–0) flux. Literature SLEDs with at least one detection at $J_{\rm upper} \geq 7$ are in thin gray/black lines (black for ALMA-observable sources; gray for northern sources). Sources lacking CO(1–0) have dashed lines; we extrapolate a CO(1–0) flux from the lowest-J measured line using average HerCULES ratios (Rosenberg *et al.* 2015). Shaded regions show envelopes of CO SLED classes identified with HerCULES: SLEDs that peak near $J_{\rm upper} \sim 4$–6 then swiftly decline which only require UV-heating from young stars (red), SLEDs that peak near $J_{\rm upper} \sim 6$–7 but do not decline as quickly which have a mixture of energy sources (yellow), and SLEDs that peak near $J_{\rm upper} \sim 9$ which *require* mechanical shock, X-ray, and/or cosmic ray heating (blue). Thermalized line ratios ($\propto J^2_{\rm upper}$) are shown in the thick black line.

The results for starburst-dominated galaxies are more mixed. While the SLEDs of SMM J14011+0252 and SMM J04431+0210 are certainly declining at higher-J (similar to the Eyelash; Danielson *et al.* 2011), BR 1202–0725 North is more highly excited than its AGN companion, perhaps due to an AGN too deeply buried in dust to have been detected by previous observations.

References

Barvainis, R., Alloin, D., Guilloteau, S., & Antonucci, R. 1998, *ApJL*, 492, L13
Bîrzan, L., Rafferty, D. A., Nulsen, P. E. J., *et al.* 2012, *MNRAS*, 427, 3468
Cañameras, R., Yang, C., Nesvadba, N. P. H., *et al.* 2018, *A&A*, 620, A61
Carilli, C. L. & Walter, F. 2013, *ARA&A*, 51, 105
Carilli, C. L., Cox, P., Bertoldi, F., *et al.* 2002, *ApJ*, 575, 145
Casey, C. M., Narayanan, D., & Cooray, A. 2014, *PhR*, 541, 45
Cicone, C., Maiolino, R., Sturm, E., *et al.* 2014, *A&A*, 562, A21
da Cunha, E., Groves, B., Walter, F., *et al.* 2013, *ApJ*, 766, 13
Danielson, A. L. R., Swinbank, A. M., Smail, I., *et al.* 2011, *MNRAS*, 410, 1687
Delvecchio, I., Gruppioni, C., Pozzi, F., *et al.* 2014, *MNRAS*, 439, 2736
Diamond-Stanic, A. M., Moustakas, J., Tremonti, C. A., *et al.* 2012, *ApJL*, 755, L26
Fabian, A. C. 2012, *ARA&A*, 50, 455
Falgarone, E., Zwaan, M. A., Godard, B., *et al.* 2017, *Nature*, 548, 430
Gallerani, S., Ferrara, A., Neri, R., & Maiolino, R. 2014, *MNRAS*, 445, 2848
Gowardhan, A., Spoon, H., Riechers, D. A., *et al.* 2018, *ApJ*, 859, 35
Harris, A. I., Baker, A. J., Zonak, S. G., *et al.* 2010, *ApJ*, 723, 1130
Ivison, R. J., Papadopoulos, P. P., Smail, I., *et al.* 2011, *MNRAS*, 412, 1913
Kereš, D., Katz, N., Weinberg, D. H., & Davé, R. 2005, *MNRAS*, 363, 2
Kirkpatrick, A., Pope, A., Sajina, A., *et al.* 2015, *ApJ*, 814, 9
Kirkpatrick, A., Sharon, C., Keller, E., & Pope, A. 2019, *ApJ*, 879, 41
Madau, P. & Dickinson, M. 2014, *ARA&A*, 52, 415
Meijerink, R., Kristensen, L. E., Weiß, A., *et al.* 2013, *ApJL*, 762, L16

https://doi.org/10.1017/S1743921319008895 Published online by Cambridge University Press

Omont, A., Petitjean, P., Guilloteau, S., *et al.* 1996, *Nature*, 382, 428
Oteo, I., Zwaan, M. A., Ivison, R. J., Smail, I., & Biggs, A. D. 2017, *ApJ*, 837, 182
Riechers, D. A., Carilli, C. L., Maddalena, R. J., *et al.* 2011, *ApJL*, 739, L32
Riechers, D. A., Bradford, C. M., Clements, D. L., *et al.* 2013, *Nature*, 496, 329
Rosenberg, M. J. F., van der Werf, P. P., Aalto, S., *et al.* 2015, *ApJ*, 801, 72
Salomé, P., Guélin, M., Downes, D., *et al.* 2012, *A&A*, 545, A57
Serjeant, S. 2012, *MNRAS*, 424, 2429
Shabala, S. S., Ash, S., Alexander, P., & Riley, J. M. 2008, *MNRAS*, 388, 625
Sharon, C. E., Riechers, D. A., Hodge, J., *et al.* 2016, *ApJ*, 827, 18
Silk, J. & Rees, M. J. 1998, *A&A*, 331, L1
Spilker, J. S., Aravena, M., Béthermin, M., *et al.* 2018, Science, 361, 1016
Stacey, H. R. & McKean, J. P. 2018, *MNRAS*, 481, L40
Swinbank, A. M., Smail, I., Longmore, S., *et al.* 2010, *Nature*, 464, 733
Thomson, A. P., Ivison, R. J., Smail, I., *et al.* 2012, *MNRAS*, 425, 2203
Tuan-Anh, P., Hoai, D. T., Nhung, P. T., *et al.* 2017, *MNRAS*, 467, 3513
van der Werf, P. P., Isaak, K. G., Meijerink, R., *et al.* 2010, *A&A*, 518, L42
Veilleux, S., Cecil, G., & Bland-Hawthorn, J. 2005, *ARA&A*, 43, 769
Weiß, A., Downes, D., Walter, F., & Henkel, C. 2007, in Astronomical Society of the Pacific Conference Series, Vol. 375, From Z-Machines to ALMA: (Sub)Millimeter Spectroscopy of Galaxies, ed. A. J. Baker, J. Glenn, A. I. Harris, J. G. Mangum, & M. S. Yun, 25
Yang, C., Omont, A., Beelen, A., *et al.* 2017, *A&A*, 608, A144

https://doi.org/10.1017/S1743921319008895 Published online by Cambridge University Press